A novel deep targeted sequencing method for minimal residual disease monitoring in acute myeloid leukemia

Esther Onecha,[1,2] Maria Linares,[1,2] Inmaculada Rapado,[1,2,3] Yanira Ruiz-Heredia,[1,2] Pilar Martinez-Sanchez,[1] Teresa Cedena,[1,2,3,4] Marta Pratcorona,[5] Jaime Perez Oteyza,[6] Pilar Herrera,[7] Eva Barragan,[4,8] Pau Montesinos,[4,8] Jose Antonio Garcia Vela,[9] Elena Magro,[10] Eduardo Anguita,[11] Angela Figuera,[12] Rosalia Riaza,[13] Pilar Martinez-Barranco,[14] Beatriz Sanchez-Vega,[1,2] Josep Nomdedeu,[5] Miguel Gallardo,[2]* Joaquin Martinez-Lopez[1,2,3,4]* and Rosa Ayala[1,2,3,4]*

[1]Hematology Department, Hospital Universitario 12 de Octubre, Madrid; [2]Hematological Malignancies Clinical Research Unit, CNIO, Madrid; [3]Centro de Investigación Biomédica en Red Cáncer (CIBERONC), Madrid; [4]Complutense University, Madrid; [5]Hematology Department, Hospital Santa Creu i Sant Pau, Barcelona; [6]Hematology Department, Hospital Universitario Sanchinarro, Madrid; [7]Hematology Department, Hospital Universitario Ramon y Cajal, Madrid; [8]Hematology Department, Hospital Universitario La Fe, Valencia; [9]Department of Hematology, Hospital Universitario de Getafe, Madrid; [10]Hematology Department, Hospital Universitario Principe de Asturias, Madrid; [11]Hematology Department, Hospital Clínico San Carlos, IdISSC, UCM, Madrid; [12]Hematology Department, Hospital Universitario de la Princesa, Madrid; [13]Hematology Department, Hospital Universitario Severo Ochoa, Madrid and [14]Hematology Department, Hospital Universitario Fundación Alcorcón, Madrid, Spain

**MG, JM-L and RA contributed equally to this work.*

 doi:10.3324/haematol.2018.194712

Received: April 2, 2018.

Accepted: August 8, 2018.

Pre-published: August 9, 2018.

Correspondence: rosam.ayala@salud.madrid.org

Supplementary data

Supplementary 1. Conditions tested during the set-up of the NGS-based method

We tested a variety of methods to find optimal conditions to detect and quantify mutations at very low allele frequency in follow-up gDNA samples.

As a first approach, we used the same conditions as those in the diagnosis protocol, with 10 ng of gDNA, selected Ampliseq primers and the Ion AmpliSeq DNA & RNA Library Preparation workflow with an expected deep coverage of 500,000 reads. In a second approach, we used a higher DNA concentration (30–50 ng), higher specificity and quality primers (TIB MOLBIOL, Roche Diagnostics, SL) with a more robust polymerase (Platinum® PCR SuperMix High Fidelity), and the "Prepare Amplicon Libraries without Fragmentation Using the Ion Plus Fragment Library Kit" (Thermo Fisher Scientific, Inc.) and its workflow, testing a wide range of internal conditions. The coverage of sequencing was increased to 1,000,000 reads, however, the sensitivity was not increased.

Supplementary 2. Conditions of the optimal NGS-based method

DNA extraction was performed in a Maxwell®16 MDx instrument (Promega Biotech Iberica, SL) and quantified on a Qubit®2.0 Fluorometer (Invitrogen™ , Thermo Fisher Scientific Inc., WA, USA).

The same primer pairs (*Supplementary Table S3*) used at diagnosis were used to amplify 0.5–1 μg of gDNA of patient samples (3 μg for calibration curve assays) by PCR using Platinum™ *Taq* DNA Polymerase High Fidelity (Invitrogen™) with the following conditions: 60 seconds at 94ºC for initial denaturation, followed by 35 cycles of 15 seconds at 94°C for denaturation, 30 seconds at 58ºC for annealing and 30 seconds at 68ºC for extension. The final volume was 100 μL (79.6 μL DNA–H_2O, 10 μL 10× High Fidelity PCR Buffer, 4 μL 50 nM MgSO4, 2 μL 10 mM dNTP Mix (NZYTech, Lda, Lisbon, Portugal), 0.4 μL DNA polymerase (5U/μL), and 2 μL each of 10 μM forward and reverse primers. Libraries were constructed using NEBNext® Fast DNA Library Prep Set for Ion Torrent™ (New England Biolabs Inc., Ipswich, MA, USA). Specificity and quantification of the final product, both for amplified DNA and amplified libraries, was analyzed with the Agilent Bioanalyser 2100 (Agilent Technologies, Palo Alto, CA, USA).

The *IDH1* and *IDH2* dilution curves allowed us established the LOD of NGS at 10^{-4}, based on mean + 2.5 SD ratio from alternative 1 and alternative 2 results (*Supplementary Table S4*). In the same way, based on mean + 2.5 SD mutated aligned reads from alternative 1 and alternative 2, a technical cutoff was established

at 70 mutated aligned reads with a minimum coverage of 100,000 readings aligned, and a prognosis value of this cutoff was validated by survival analyses (*Supplementary Figure S3*).

Supplementary 3. Digital PCR of *NMP1* and *IDH1/2* mutations

dPCR for 10-fold dilutions curves of *NPM1*, *IDH1* and *IDH2* mutated gDNA was performed with specific primers and probes. Allele frequency was calculated as the ratio of mutated copies to wild-type copies/µL. dPCR assays were performed using QuantStudio™ 3D Digital PCR System using the FAM™/VIC® TaqMan® Assay (Applied Biosystems™, Thermo Fisher, La Jolla CA, USA) to study *NPM1* type A (c.863_864insTCTG), *IDH1* (c.394C/T) and *IDH2* (c.515G/A). A final volume of 14.5 µL (7.5 µL of PCR Master Mix 2×, 0.75 µL TaqMan® Assay 20× and 6.75 µL of gDNA at 50 ng/µL) was loaded into a QuantStudio™ 3D Digital PCR Chip v2 (Thermo Fisher), and amplified by PCR using the GeneAmp® 9700 system (Thermo Fisher). PCR was performed with the following conditions: 10 minutes at 96ºC for initial denaturation, 39 cycles of 2 minutes at 56–60ºC followed by 30 seconds at 98ºC, and a final 2 minutes step at 60ºC. After the PCR, each chip was read individually using the QuantStudio™ 3D Digital PCR Instrument (Thermo Fisher Scientific, Inc), which generates a file (.eds) containing the processed image data that is then interpreted using QuantStudio™ 3D AnalysisSuite Software (Thermo Fisher Scientific, Inc).

Supplementary 4. MRD monitoring of *NMP1* by qPCR

Detection and quantification of mutated *NPM1* transcripts were performed by allele-specific qPCR according to the procedure described by Gorello,[1] using RNA as starting sample. The protocol to detect *NPM1* by RT-PCR was performed in a final volume of 10 µl: 1.5 µL of H_2O + 0.5 µL of cProbe-LNA 4 µM (5´- 6FAM-ACCAAGAGGCT+A+T+TC+A+A– –BBQ -3´, Isogen Life Science) + 0.5 µL cNPM-F (10 µM, Isogen Life Science), 5´-GAAGAATTGCTTCCGGATGACT-3´+ 0.5 µL cNPM–mutA-R (10 µM, Isogen Life Science), 5´-CTTCCTCCACTGCCAGACAGA-3´+ 5 µL of Taq Man Fast Advanced Master Mix (Applied Biosystems) + 2 µL of cDNA. Amplification conditions were: 2 min at 50ºC for enzyme activation, 20 seconds at 95ºC for initial enzyme inactivation and AmpliTaq polymerase activation, followed by 40 cycles of 60 seconds at 95ºC for denaturation plus 20 seconds at 60ºC for annealing. We used the ABI PRISM 7900 Sequence Detection System (Applied Biosystems) for sample amplification and analysis.

For normalization of the expression of mutated *NPM1*, *GUS-β* expression was used as a control. MRD positive status was considered as the presence of *NPM1* copies > 0.00001 after therapy.[2]

Supplementary 5. MRD monitoring by MFC

After erythrocyte lysis, follow-up bone marrow samples were analyzed using a panel of monoclonal antibodies for the detection of the same immunophenotypic alterations described at diagnosis.[3] In our study, 10/75 (13%) samples evaluated by MCF were determined with MCF of 8 colours and the remaining 65/75 (87%) were determined with MCF of 4 colours. MRD positive status by flow cytometry was considered as the presence of AML cells greater than 0.001 at post-therapy.[2]

Supplementary 6. Statistical analyses

Contingency tables were used to analyse associations between categorical variables using Fisher´s test or Chi-square test for statistical significance. Student´s t-test was used to compare averages of continuous variables between groups. The concordance between sequencing, MFC and qPCR was analysed in log space using the Spearman correlation test. ROC (receiver operating characteristic) curves were employed to establish the cutoff value to predict survival by the NGS method, by MFC or by qPCR; however, for MFC and qPCR, the sensitivity and specificity achieved were comparable or less than those using the standard thresholds for MRD detections in AML and finally we used these (data not shown). For survival analysis, the endpoints examined were disease-free survival (DFS) and overall survival (OS), from the starting point of the treatment. In the cases that several samples from the same patient were evaluated, the one in which the lowest MRD levels were detected was selected for survival analysis. Survival curves were calculated according to the Kaplan-Meier method, and the log-rank test was used for estimation of survival and differences between groups. Univariate and multivariate analysis were performed using the Cox regression model; the most relevant variables for univariate analysis were: sex, age, blasts at diagnosis, leukocytes at diagnosis, cytogenetic risk (ELN recommendation; groups: favorable, intermediate and adverse), mutated *FLT3*-ITD, hematopoietic stem cell transplantation (HSCT) (groups: allo-HSCT, auto-HSCT and therapy), and MRD status by each technique (MFC, qPCR, NGS). Variables included in the multivariate analysis were chosen based on the results obtained in the univariate analysis and those with greater prognostic relevance in AML: sex, age, leukocytes at diagnosis, cytogenetic risk, mutated *FLT3*-ITD and MRD status by NGS.

Statistical analysis was performed using the R statistical software platform. All p values were two-sided, with statistical significance defined as a p–value of 0.05 or less.

Supplementary Table S1. Samples and patients evaluated.

Follow-up samples included in the study and their correlation patient, as well as evaluation time. In those

patients where a single sample was studied the patient is noted with the letter M. If several samples were studied per patient, these are listed numerically (M1, M2, etc.), and the sample selected for the analysis of survival is indicated. The levels of MRD in P3, P9, P38 and P62 patients were evaluated by studying both *NPM1* and *IDH1*. The sample selected for survival analysis is indicated. Two patients were removed from the study because of a missed follow-up.

Supplementary Table S2. Genes included in the NGS panel

Genes sequenced by NGS grouped by biological function, the chromosome where it is located, genomic coordinates (start–end) of region sequenced, the number of amplicons that the gene covers, the region of the gene that encompasses all the amplicons expressed as a percentage, and the number of exons.

Supplementary Table S3. Sequences of primers for MRD assay

Specific primer sequences (TIB MOLBIOL, Roche Diagnostics, SL) taken from the custom AML panel used at diagnosis (Ion AmpliSeq™, Thermo Fisher Scientific, Inc) for *DNMT3A* (used only for optimization), *IDH1*, *IDH2,* and *FLT3*; or from the commercial panel (Ion AmpliSeq™ AML Panel) in the case of *NPM1*.

Supplementary Table S4. VAF of dilution curves

Table represents the counts of aligned reads, both of the target sequence, wt sequence and the other two possible alternatives (sequences not mutated), the ratio (mutated aligned sequences/wt aligned sequences), and the fluctuation of the ratio with respect to the mutated sequence [Δlog(ratio)]; according to *IDH1* **(A)** and *IDH2* dilution curves **(B).** The LOD (10^{-4}) was established based on ratio mean + 2.5 SD from alternative 1 and alternative 2 results.

Supplementary Figure S1. ROC curves

Plots show the sensitivity or true positive rate (TPR) in the y-axis against 1-specificity or the false positive rate (FPR) in the x-axis, at various threshold settings. ROC curves determined the optimal cutoff level that maximizes sensitivity and specificity for the cases evaluated at each check-point for both OS and DFS studies. For OS the sensitivity and the specificity achieved was 0.69 and 0.77 at post-induction, 0.73 and 0.91 at post-consolidation, and 0.71 and 0.67 at both together. For DFS the sensitivity and the specificity

achieved was 0.77 and 0.60 at post-induction, 0.76 and 0.89 at post-consolidation, and 0.72 and 0.67 at both together. The area under the curve (AUC) is annotated.

Supplementary Figure S2. Correlation of levels of MRD measure by NGS and conventional methods

Correlation between NGS *vs* MFC (left) and correlation between NGS *vs* qPCR (right) detected by Spearman test; cases with available data for these tests were included. A significant positive correlation were found in both cases: NGS *vs* MFC (r=0.41, p=0.003), and NGS *vs* qPCR (r=0.46, p<0.001).

Supplementary Figure S3. Prognostic value of technical cutoff

A, OS curves of patients stratified according to MRD status based on technical cutoff (70 aligned mutated reads). The group categorized as MRD negative had greater OS than the group categorized as MRD positive (HR: 2.55 (1.00–6.46), p=0.049). **B,** DFS curves of patients stratified under same criteria, the MRD negative group had greater DFS than the group categorized as MRD positive (HR: 3.18 (1.16–8.69), p=0.024. Number of censored patients with respect to the stratified groups and the number at risk is indicated. *P values are considered significant (< 0.05), ** (< 0.01).

References

1. Gorello P, Cazzaniga G, Alberti F, Dell'Oro MG, Gottardi E, Specchia G, et al. Quantitative assessment of minimal residual disease in acute myeloid leukemia carrying nucleophosmin (NPM1) gene mutations. Leukemia. 2006;20(6):1103-8.

2. Schuurhuis GJ, Heuser M, Freeman S, Bene MC, Buccisano F, Cloos J, et al. Minimal/measurable residual disease in AML: a consensus document from the European LeukemiaNet MRD Working Party. Blood. 2018;131(12):1275-91.

3. Tomlinson B, Lazarus HM. Enhancing acute myeloid leukemia therapy - monitoring response using residual disease testing as a guide to therapeutic decision-making. Expert Rev Hematol. 2017;10(6):563-74.

Onecha.E et al.
Supplementary Table S1.

Patient	Marker	1I		2I	1C		2C		3C			Selected Sample		
P1	NPM1	M1	**M2**				M3					M2		
P2	NPM1	**M1**			M2		M3					M1		
P3	NPM1	**M1**					M2					M1		
	IDH1	M										–		
P4	NPM1	**M1**			M2							M1		
P5	NPM1	**M1**			M2		M3					M1		
P6	NPM1	**M1**							M2			M1		
P7	NPM1	**M**										M		
P8	NPM1	**M**										M		
P9	IDH1	M										–		
	NPM1	**M**										M		
P10	NPM1	**M**										M		
P11	NPM1	**M**										M		
P12	NPM1	**M1**			M2							M1		
P13	NPM1	**M**										M		
P14	NPM1	**M**										M		
P15	IDH2	**M**										M		
P16	NPM1	**M**										M		
P17	NPM1	M1	**M2**									M2	Induction (n=35)	Survival Analysis (n=63)
P18	NPM1	**M**										M		
P19	NPM1	**M**										M		
P20	NPM1	**M**										M		
P21	NPM1	**M**										M		
P22	NPM1	**M**										M		
P23	NPM1	**M**										M		
P24	NPM1	**M**										M		
P25	NPM1	**M**										M		
P26	NPM1	**M**										M		
P27	FLT3			**M**								M		
	NPM1			M								M		
P28	IDH2	**M**										M		
P29	NPM1	**M**										M		
P30	FLT3	**M**										M		
P31	NPM1	**M**										M		
P32	NPM1	**M**										M		
P33	NPM1	**M**										M		
P34	NPM1	**M**										M		
P35	NPM1	**M1**			M2		M3					M1		
P36	IDH1				M1	**M2**						M2		
P37	NPM1	M1							M2			M2		
P38	IDH1						**M1**		M2			M1		
	NPM1						M1		M2			–		
P39	IDH2						M1		M2	M3	**M4**	M4		
P40	NPM1								**M1**	M2		M1		
P41	NPM1	M1			**M2**							M2		
P42	NPM1				**M1**				M2			M1		
P43	NPM1						M1	**M2**				M2		
P44	NPM1	M1							**M2**			M2		
P45	NPM1	M1							**M2**			M2		
P46	NPM1	**M1**							M2			M1		
P47	NPM1								**M**			M		
P48	NPM1								**M**			M		
P49	NPM1	**M1**			M2							M1	Consolidation (n=28)	
P50	NPM1								**M**			M		
P51	NPM1								**M**			M		
P52	NPM1				**M**							M		
P53	IDH2								**M**			M		
P54	NPM1								**M**			M		
P55	NPM1								**M**			M		
P56	NPM1	M1			**M2**							M2		
P57	NPM1				**M**							M		
P58	NPM1				**M**							M		
P59	NPM1	M1			**M2**		M3					M2		
P60	NPM1	M1			**M2**							M2		
P61	NPM1				**M**							M		
P62	IDH1	M1					**M2**					M2		
	NPM1	M1					M2					–		
P63	NPM1	M1			**M2**							M2		
–	NPM1	M1			M2							–		
–	NPM1								M			–		
		n=51			n=55									
		n = 106												

Onecha.E et al.
Supplementary Table S2.

	Gene	Chr	Start	End	Amplicons	Coverage (%)	Exons
Trancription factor	ETV6	Chr 12	11802955	12044078	20	94	8
	RUNX1	Chr 21	36164534	36421235	18	69	10
Signaling molecular	EPOR	Chr 19	11488599	11495009	21	93	8
	FLT3	Chr 13	28578144	28644774	53	97	24
	HRAS	Chr 11	532519	534348	10	83	5
	JAK2	Chr 9	5021946	5126885	57	97	23
	SH2B3	Chr 12	111855922	111886159	15	64	7
Epigenetic Regulation	DNMT3A	Chr 2	25457019	25523119	51	91	25
	IDH1	Chr 2	209101751	209116313	22	98	8
	IDH2	Chr 15	90627407	90634952	21	87	11
	TET2	Chr 4	106155047	106197701	64	99	10
	ASXL1	Chr 20	30954090	31025087	52	91	13
	KDM6A	Chr X	44732713	44970702	64	93	29
	KMT2A	Chr 11	118339409	118392930	145	96	37
	MPL	Chr 1	43803438	43818424	30	92	12
	PHF6	Chr X	133511597	133559416	22	98	11
Transciptional regulation	CBL	Chr 11	119077153	119170540	41	93	16
	EZH2	Chr 7	148504653	148544423	44	99	21
	KIT	Chr 4	55524151	55604786	51	99	22
	KRAS	Chr 12	25362621	25398385	10	83	5
	NRAS	Chr 1	115251095	115258874	9	100	4
	CALR	Chr 19	13049314	13055076	23	86	9
Splicing	SF1	Chr 11	64532722	64545911	30	80	19
	SF3A1	Chr 22	30730553	30752852	37	94	18
	SF3B1	Chr 2	198256947	198299851	66	97	26
	SRSF2	Chr 17	74732208	74733231	5	70	2
	U2AF35	Chr 21	44513107	44524598	15	87	10
	ZRSR2	Chr X	15808511	15841407	26	97	11
	PRPF40B	Chr 12	50024310	50037977	54	95	26
Tumor supressor	PTEN	Chr 10	89624161	89725315	21	93	9
	TP53	Chr 17	7572847	7579960	21	93	13
	VHL	Chr 3	10183314	10195319	27	55	3

Onecha.E et al.
Supplementary Table S3.

GENE	PRIMERS
IDH1	Fw, 5´–AAGAATAAAACACATACAAGTTGGAAATTTCT–3´
	Rv, 5´–GAGAAGCCATTATCTGCAAAAATATCCC–3´
IDH2	Fw, 5´–ACAAAGTCTGTGGCCTTGTACTG–3´
	Rv, 5´–CTGGACCAAGCCCATCACCAT–3´
NPM1	Fw, 5´–GTTAACTCTCTGGTGGTAGAATGAAAAATAGA–3´
	Rv, 5´–GATATCAACTGTTACAGAAATGAAATAAGACG–3´
FLT3	Fw, 5´– TTGGAAACTCCCATTTGAGATCATATTCAT–3´
	Rv, 5´–TCTATCTGCAGAACTGCCTATTCCTAA –3´
DNMT3A	Fw, 5´–GATGACTGGCACGCTCCAT–3´
	Rv, 5´–GCTGTGTGGTTAGACGGCTTC–3´

Onecha.E et al.
Supplementary Table S4.

A) IDH1 Dilution Curve

		Mutated sequence (c.515G>A)			Alternative sequence 1 (c.515 G>T)				Alternative sequence 2 (c.515 G>C)			
Dil	Aligned wt Reads	Aligned Mutated Reads	Ratio	log(ratio)	Aligned Alt.1 Reads	Ratio	log(ratio)	Δlog(ratio) $_{alt1\text{-}mut}$	Aligned Alt.2 Reads	Ratio	log(ratio)	Δlog(ratio) $_{alt2\text{-}mut}$
1	46,955	1,198,507	2.55^{1}	1.41	50	1.06^{-3}	-2.97	-4.38	57	1.21^{-3}	-2.92	-4.32
10^{-1}	1,346,647	100,279	7.45^{-2}	-1.13	19	1.41^{-5}	-4.85	-3.72	6	4.46^{-6}	-5.35	-4.22
10^{-2}	1,716,364	11,065	6.45^{-3}	-2.19	44	2.56^{-5}	-4.59	-2.4	1	5.83^{-7}	-6.23	-4.04
10^{-3}	1,987,343	1,958	9.85^{-4}	-3.01	30	1.51^{-5}	-4.82	-1.81	1	5.03^{-7}	-6.3	-3.29
10^{-4}	1,607,631	368	2.29^{-4}	-3.64	35	2.18^{-5}	-4.66	-1.02	0	0	–	–
10^{-5}	2,100,916	341	1.62^{-4}	-3.79	35	1.67^{-5}	-4.78	-0.99	0	0	–	–
10^{-6}	1,532,477	223	1.46^{-4}	-3.84	19	1.24^{-5}	-4.91	-1.07	0	0	–	–
Control	1,399,100	268	1.92^{-4}	-3.72	19	1.36^{-5}	-4.87	-1.15	1	7.15^{-7}	-6.15	-2.43

B) IDH2 Dilution Curve

		Mutated sequence (c.394 C>T)			Alternative sequence 1 (c.394 C>A)				Alternative sequence 2 (c.394 C>G)			
Dil	Aligned wt Reads	Aligned Mutated Reads	Ratio	log(ratio)	Aligned Alt.1 Reads	Ratio	log(ratio)	Δlog(ratio) $_{alt1\text{-}mut}$	Aligned Alt.2 Reads	Ratio	log(ratio)	Δlog(ratio) $_{alt2\text{-}mut}$
1	179,315	199,266	1.11	0.05	6	3.35^{-5}	-4.48	-4.52	4	2.23^{-5}	-4.65	-4.70
10^{-1}	319,918	24,128	7.54^{-2}	-1.12	5	1.56^{-5}	-4.81	-3.68	0	–	–	–
10^{-2}	369,661	2,687	7.26^{-3}	-2.14	2	5.41^{-6}	-5.27	-3.13	1	2.71^{-6}	-5.57	-3.43
10^{-3}	330,661	372	1.12^{-3}	-2.95	2	6.05^{-6}	-5.22	-2.27	0	0	–	–
10^{-4}	222,345	120	5.39^{-4}	-3.27	2	9.00^{-6}	-5.05	-1.78	0	0	–	–
10^{-5}	288,670	348	1.21^{-3}	-2.92	5	1.73^{-5}	-4.76	-1.84	0	0	–	–
10^{-6}	411,045	265	6.45^{-4}	-3.19	8	1.95^{-5}	-4.71	-1.52	0	0	–	–
Control	391,770	423	1.08^{-3}	-2.97	6	1.53^{-5}	-4.81	-1.85	1	2.55^{-6}	-5.59	-2.63

Onecha.E et al.
Supplementary Figure S1.

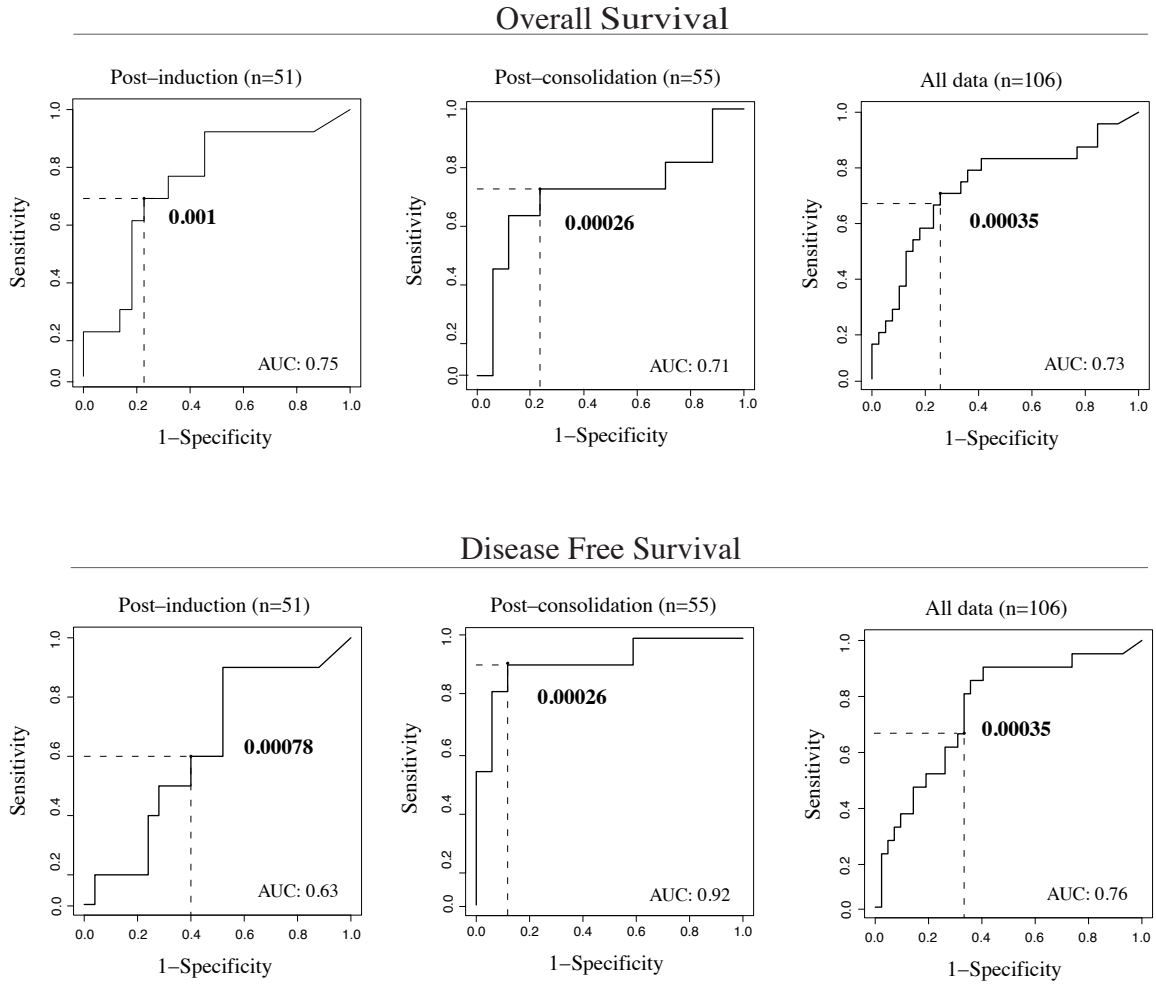

Onecha.E et al.
Supplementary Figure S2.

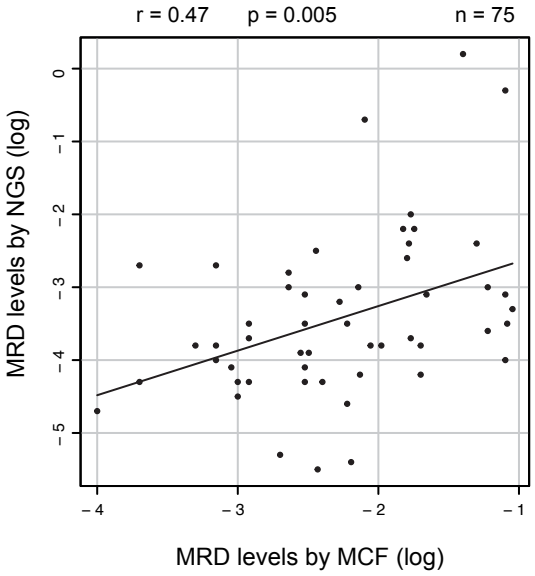

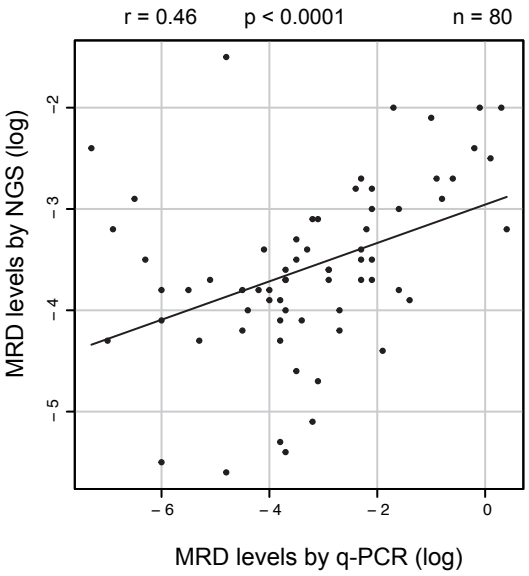

Onecha.E et al.
Supplementary Figure S3.